Opto-Electronics Review

journal homepage: https://journals.pan.pl/opelre

Organic *vs.* standard photodetectors (Mini Review)

Antoni Rogalski[1*], Fang Wang[2], Weida Hu[2], Piotr Martyniuk[1]

[1] Institute of Applied Physics, Military University of Technology, ul. gen. Sylwestra Kaliskiego 2, 00-908 Warsaw, Poland
[2] State Key Laboratory of Infrared Physics, Shanghai Institute of Technical Physics, Chinese Academy of Sciences, 500 Yu Tian Road, Shanghai 200083, China

Article info

Article history:
Received 01 Dec. 2024
Received in revised form 08 Jan. 2025
Accepted 09 Jan. 2025
Available on-line 25 Feb. 2025

Keywords:
organic photodetectors;
signal fluctuation limit;
BLIP limit;
overestimation of performance.

Abstract

Organic semiconductors (OSCs) have been found to be a prominent group of optoelectronic materials extensively researched for more than 40 years due to their ability to tune capabilities by modifying chemical structure and simple processing. Their performance has been significantly improved, advancing from the fast development in the design and synthesis of new OSC materials. This paper attempts to essentially confront the performance of organic photodetectors with standard detectors dominating the global commercial market. Special attention was paid to the organic field-effect transistor (FET) phototransistors detectivity overestimates.

1. Introduction

Organic semiconductors (OSCs) have been of great interest for more than 40 years, exhibiting the potential to transform significant technologies, such as photovoltaic energy, transparent screens/displays, efficient and reasonably priced white lighting or flexible and robust electronics [1–10], however, most efforts have been directed on lighting/display development. The unique properties also make them suitable for photodetectors with spectral responsivity ranging from ultraviolet (UV) to near infrared (NIR) with the panchromatic or selective tuning of specific wavelengths [6, 8, 10].

Research on organic materials has been driven by technological superiority over inorganic semiconductors (ISCs) which include Si, Ge, GaN, GaAs, and InGaAs. Compared to the latter, organic compounds are generally cheap and match large areas, low temperatures, and low-cost fabrication methods (compatible with high-throughput roll-to-roll processing). In addition, majority of inorganic materials require high-quality substrates, while in contrast due to high lattice mismatch tolerance and deformation-induced defect states, organic devices are fabricated on plastic films, metal foils or glass.

Despite their many advantages, organic materials also have disadvantages. One of the fundamental ones is the low carriers mobility, which is related to the weak inter-molecular interactions, reducing performance compared to inorganic devices. In addition, the majority of organic materials are found not to be very stable, they are susceptible to degradation by water vapour and oxygen exposure and require special housing to reach satisfactory device durability. Another problem is related to the purity of organic materials – much lower than that of inorganic materials, with the consequent creation of electronic defects reducing device performance.

This paper compares the performance of organic photodetectors with standard detectors dominating the global commercial market. Special attention was paid to the organic field-effect transistor (FET) phototransistors detectivity overestimates and the reasons for these overestimates were explained.

2. Fundamental detectivity limits

The photon detectors perform best when the detector internal noise is below the photon noise [11–13]. The level of photon noise is not connected with the imperfections of the detector design or the integrated electronics but is conditioned by the electromagnetic radiation field discrete

*Corresponding author at: antoni.rogalski@wat.edu.pl

https://doi.org/10.24425/opelre.2025.153812
1896-3757/ Association of Polish Electrical Engineers (SEP) and Polish Academic of Sciences (PAS). Published by PAS

nature. The radiation interacting with the device includes two components originating from the target and the surrounding background. Therefore, there are two fundamental limitations to the device performance, resulting from the target signal fluctuation limitation (SFL) and the influence of the ambient scene radiation – background limited infrared photodetector (BLIP). The SFL and BLIP detectivities defining these limits are shown in Fig. 1 in the spectral range of 0.2–2 µm. As shown, the intersection of the SFL and BLIP curves occurs at a wavelength, l ~ 1.2 µm. For < 1.2 µm, the ultimate detectivity is weakly wavelength dependent; however, for > 1.2 µm, where BLIP dominates, the $D^*(\lambda)$ dependence is strong, which results from an intensive increase of the background radiation influence at the edge of the ambient spectral distribution at 300 K.

Figure 1 also compares OSC photodetectors detectivity (D^*) with selected standard photon detectors dominating the global market and operating at 300 K for 2π field of view (FOV). More information on the OSC photodetectors (also classified by fabricating methods) is summarized in Table 1 of the paper by authors Wang *et al*. [14] and highlighted by the pink area in Fig. 1. The upper detectivities of OSC photodetectors match well with the typical values for standard detectors. However, the spread of these values is about three orders of magnitude conditioned by the immature state of technology. In the case of standard detectors, AlGaN photodiodes show the highest D^* at 260 nm, but to achieve high D^* close to the SFL limit, it is essential to use filters to reduce the contribution of residual solar radiation [15]. The record detectivity above 10^{15} Jones marked with magenta for OSC UV photodetectors [16–19] is overestimated. It should be

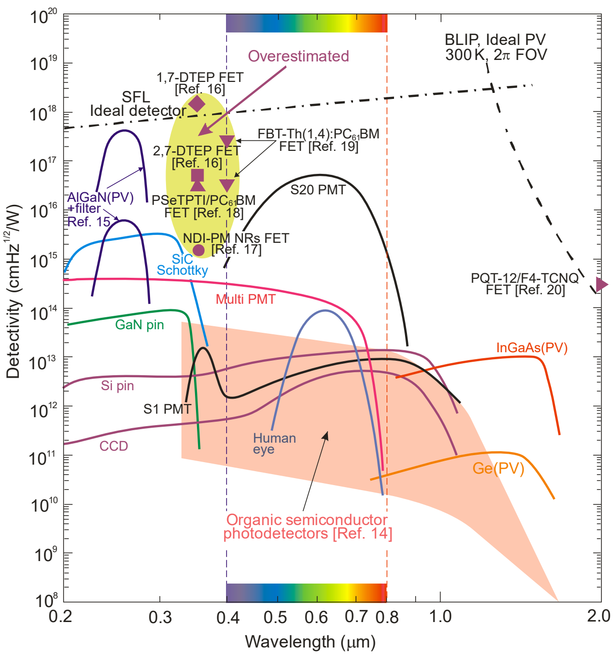

Fig. 1. Comparison of room temperature D^* for OSC photodetectors [14, 16–20] with standard market detectors (AlGaN, Si, Ge, InGaAs PDs, and PMTs) in the wavelength range of 0.2–2 µm. The ultimate SFL and BLIP are also shown. PV – photovoltaic detector, PMT – photomultiplier tube, FET – field-effect transistor. The OSC photodetectors D^* marked in magenta are overestimated.

emphasized that in this case no information is provided about the use of filters in the photodetectors performance measurements. Also, the data from [20] taken for the NIR FET phototransistor ($\lambda = 2$ µm) is overestimated (above BLIP limit).

There are several reports highlighting the overestimated performance imperfect characterization procedures, including [21–24]: (*i*) incorrect noise estimates, (*ii*) device active area and radiant power density miscalculation, (*iii*) contradiction between measured sensitivity and noise bandwidth (BW), and (*iv*) poor linear dynamic range (LDR) of the photodetectors (inapplicable to intense light due to the small volume of the active area despite a large absorption coefficient). The appropriate measurement procedures consistent with those used for typical bulk-based photodetectors are required. Probably the main reason for the D^* overestimates reported in [16–20] (record > 10^{18} Jones [17]) is the failure to include the photogating effect, *g*, in the measurements of the shot noise and the generation-recombination (g-r) noise. Assuming incorrect ($I_{sh} = \sqrt{2qI\Delta f}$) expression for the shot noise (proper $I_{sh} = \sqrt{2qgI\Delta f}$) leads to the false improvement in the signal-to-noise ratio (SNR) by a factor of $\sqrt{g}$. A similar dependence on $\sqrt{g}$ can be found for frequency-related (ω) g-r noise according to the relation $I_{gr} = \sqrt{4qI_d g\Delta f/(1+\omega^2\tau^2)}$.

3. Performance of OSC photodetectors

Published reviews on OSC advances cover different topics, including organic materials, device designs, physics, processing, and applications [6–8, 10, 14, 25, 26]. The literature on the subject contains a huge amount of data on the materials used, the design of the devices, and their characteristics. The main modes of operation of OSC photodetectors are photoconductive (PC), photovoltaic (PV), and FET photodetectors.

Most OSCs-based photodetectors are processed as photodiodes reaching internal quantum efficiency (IQE) < 100%. The avalanche effect does not occur in OSCs (relatively high binding energy of the excitons) to increase their sensitivity. Generally, the photodiodes exhibit a very low power dissipation, negligible 1/*f* noise, inherently high impedance, and easy multiplexing via readout integrated circuits (ROICs) and are normally used for large numbers of pixel arrays. The reverse-biased photodiodes reach high impedance and may match better electrically into low-noise/compact silicon readout preamplifier circuits. The photoresponse is linear for much higher photon flux than for photoconductors, mainly due to higher doping levels of the absorber region and rapid photogenerated carriers collected by the junction electric field.

The high detector performance requires low (as much as possible) dark current density. Compared with ISC standard photodiodes, the OSCs-based photodiodes exhibit higher dark current than predicted for thermally generated radiative transitions. Sandberg *et al*. reported (based on an analysis of the temperature-dependent dark current characteristics of the OSC blend photodiodes) that the thermal activation of the dark current for low reverse bias is consistent with transitions via the mid-gap states [27].

If the dark saturation current of photodiodes is fundamentally limited by mid-gap trap states, the dark current component can be expressed by $J_d = J_0[\exp(qV/mkT) - 1]$, where J_0 corresponds to the dark current saturation density, m is the diode ideality factor. In the case of mid-gap states $m = 2$. Figure 2(a) presents the dark current density trends for large set of photodiodes. It is clearly shown that in the region of the larger energy gap (greater than 0.7 eV), the dark current density of OSC photodiodes is higher than that of standard photodiodes (Si, GaAs, and CdTe) and is limited by the g-r current in the depletion region.

Figure 2(b) shows the estimated upper limit of detectivity for the set of OSC photodiodes. The mid-gap states appear to have a decisive influence on the spectral dependence of the detectivity (red line), which is, however, well below the BLIP limit.

Another structure is the organic FET. The FET phototransistor is a three-terminal device (i.e., drain, gate, source electrodes) where the gate voltage can adjust the channel resistance (between the source and drain). Furthermore, the transport channel can also be modulated by the light absorption in OSC generating carriers. As a result, the phototransistor exhibits high photocurrent and high responsivity, as well as high internal photoconductive gain leading to photocurrent enhancement and external quantum efficiency (EQE) > 100%. Channel material should exhibit both high efficient light absorption and carrier mobility to reach high photosensitivity. Progress has been made through designing molecular structures and modifying the film morphologies. Table 1 collects the record-breaking performance of OSCs phototransistors. Detectivities are also highlighted in Fig. 1 [16–20], where some reported results are unrealistic, being close to or even exceeding the fundamental SFL and BLIP limits, SFL [16] and BLIP [20].

The existence of a large photogating effect in organic phototransistors affects the ability to achieve high current responsivity. The responsivity improvement by the photogating effect leads to the LDR caused by the charge relaxation time. The response times can reach up to several seconds, as shown in Table 1 [18].

EQE is often used as the key figure of merit to determine the performance of photoconductors and phototransistors. Since the current responsivity is given by the formula $R = (q\lambda\eta/hc)g = (q\lambda/hc)\text{EQE}$; it follows that $\text{EQE} = \eta g$. These considerations also show that an increase in quantum efficiency above 100% (when the gain, g, is above 1) results from an enhancement of photoconductive gain (in FET phototransistors – photogating effect), which reaches a value of up to about $g \sim 10^6$ at low excitation levels (see Fig. 3). It is supposed that the large value of photoconductivity gain in FET phototransistors, not considered in the shot and g-r noises estimate, is the reason

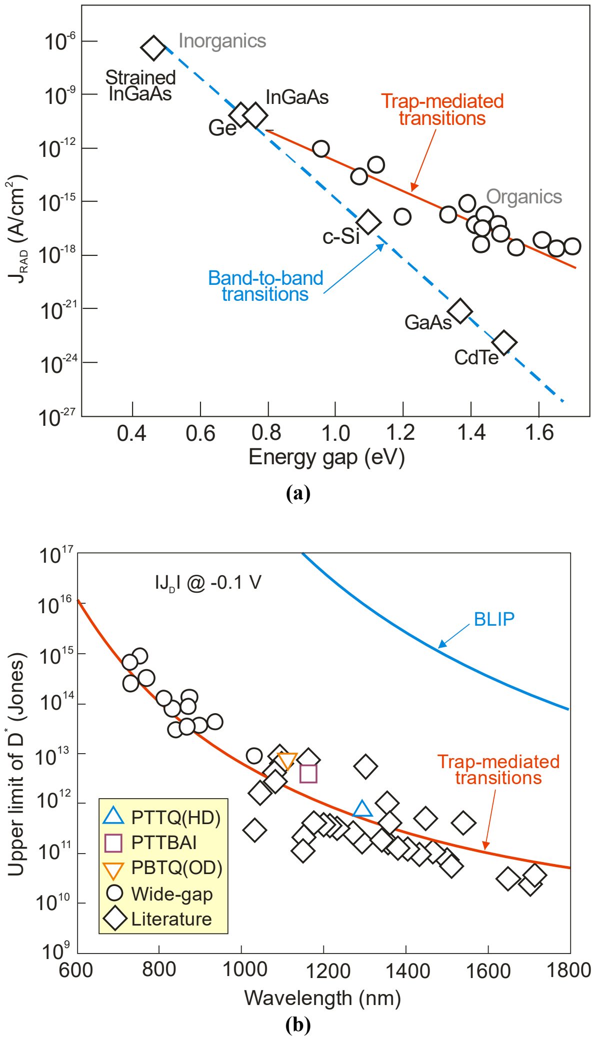

Fig. 2. Influence of mid-gap trap states on the performance of OSC based photodiodes: (a) dark current densities trends (triangles, square, and circles are from [27]; ◇ – from the selected published papers); (b) the estimated upper limit (red line) of detectivity (after [27]).

Table 1.
Record performance of organic FET phototransistors.

Material	Wavelength [nm]	Responsivity [A/W]	g/EQE [%]	Detectivity [Jones]	Response time	Ref.
2,7-DTEP	370	1.04×10^5	–	5.28×10^{16}	–	[16]
1,6-DTEP	370	2.86×10^6	–	1.49×10^{18}	–	[16]
NDI-PM NRs	365	7.23×10^3	$–/2.5 \times 10^6$	1.4×10^{15}	≈ 250 ms	[17]
PSeTPTI/PC_{61}BM	365	2.2×10^4	$7.5 \times 10^4/–$	3.1×10^{16}	≈ 3 s	[18]
FBT-Th4(1,4):PC61BM	410	1.2×10^5	$3.7 \times 10^5/–$	3.18×10^{16}	≈ 300 ms ($V_G = 30$ V)	[19]
FBT-Th4(1,4):PC61BM	410	1.6×10^4	$5.0 \times 10^4/–$	3.3×10^{17}	≈ 40 ms ($V_G = 0$ V)	[19]
PQT-12/F4-TCNQ	2000	2.75×10^6	$–/10^8$	3.12×10^{14}	≈ 10 ms	[20]

for the overestimation of the detectivity of organic photodetectors.

For comparison, Figure 3 shows a typical range of detectivity and current sensitivity of standard photodetectors (photodiodes) for 350–1500 nm. In general, in the high *g* range, the detectivity of FET phototransistors is much higher than that of standard photodetectors. The experimental data marked in the grey box are overestimated.

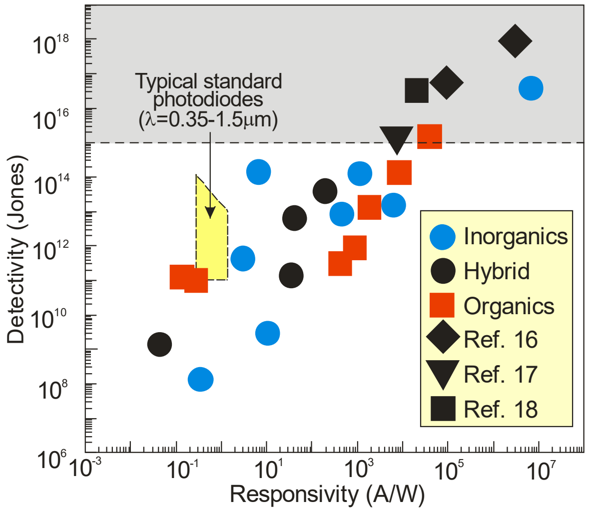

Fig. 3. Detectivity *vs*. current responsivity for visible-blind UV photodetectors presented in [17] and taken from [16] and [18]. The experimental data above the dashed line (in the grey box) are overestimated.

4. Conclusions

OSC materials emerged from a niche research topic as a promising alternative to photodetector applications, especially in the photovoltaic market. Their performance has been dramatically improved in the spectral range from UV to NIR.

OSCs are low-cost and evidently more ecological than ISCs, even if their inherent electrical properties cause performance limitations. One of the fundamental ones is the low mobility of charge carriers due to weak intermolecular interactions. In addition, most of these materials are not very stable.

The estimated upper limit of detectivity for OSC photodiodes is comparable to standard inorganic compounds. The spread of these values is about three orders of magnitude which is conditioned by the immature state of technology. Furthermore, many papers report detectivity > 10^{15} Jones, indicating they are overestimated. The record-breaking performance of OSC photodetectors, mainly phototransistors, published in the literature (exceeding SFL and BLIP limits) is related to the erroneous estimates of parameters.

Acknowledgements

This paper was supported by the Polish National Science Centre within Project UMO-2021/41/B/ST7/ 01532.

References

[1] Peumans, P., Yakimov, A. & Forrest, S. R. Small molecular weight organic thin-film photodetectors and solar cells. *J. Appl. Phys*. **93**, 3693–3723 (2003). https://doi.org/10.1063/1.1534621

[2] Forrest, S. F. The path to ubiquitous and low-cost organic electronic appliances on plastic. *Nature* **428**, 911–918 (2004). https://doi.org/10.1038/nature02498

[3] Shaheen, S. E., Ginley, D. S. & Jabbour, G. E. Organic based photovoltaics: Toward low-cost power generation. *MRS Bull*. **30**, 10–19 (2005). https://doi.org/10.1557/mrs2005.2

[4] Scott, J. C. & Bozano, L. D. Nonvolatile memory elements based on organic materials. *Adv. Mater*. **19**, 1452–1463 (2007). https://doi.org:10.1002/adma.200602564

[5] Xue, J. Perspectives on organic photovoltaics. *Polym. Rev*. **50**, 411–419 (2010). https://doi.org/10.1080/15583724.2010.515766

[6] Baeg, K.-J., Binda, M., Natali, D., Caironi, M. & Noh, Y.-Y. Organic light detectors: Photodiodes and phototransistors. *Adv. Mater*. **25**, 4267–4295 (2013). https://doi.org/10.1002/adma.201204979

[7] Manousiadis, P. P., Yoshida, K., Turnbull, G. A. & Samuel, I. D. W. Organic semiconductors for visible light communications. *Philos. Trans. R. Soc*. *A* **378**, 20190186 (2020). https://doi.org/10.1098/rsta.2019.0186

[8] Simone, G., Dyson, M. J., Meskers, S. C. J., Janssen, R. A. J. & Gelinck, G. H. Organic photodetectors and their applications in large area and flexible image sensors: The role of dark current. *Adv. Funct. Mater*. **30**, 1904205 (2019). https://doi.org/10.1002/adfm.201904205

[9] Forrest, S. R. *Organic Electronics: Foundations to Applications*. (Oxford University Press, 2020).

[10] Ren, H., Chen, J.-D., Li, Y.-Q. & Tang, J.-X. Recent progress in organic photodetectors and their applications. *Adv. Sci*. **8**, 2002418 (2020). https://doi.org/10.1002/advs.202002418

[11] Kruse, P. W. The Photon Detection Process. in *Optical and Infrared Detectors* (ed. Keyes, R. J.) 5–69 (Springer, Berlin, 1977).

[12] Kingston, R. H. *Detection of Optical and Infrared Radiation*. (Wiley, New York, 1983).

[13] Dereniak, E. L. & Boremen, G. D. *Infrared Detectors and Systems*. (Wiley, New York, 1996).

[14] Wang, Y. *et al*. Narrowband organic photodetectors – towards miniaturized, spectroscopic sensing. *Mater. Horiz*. **9**, 220–251 (2022). https://doi.org/10.1039/D1MH01215K

[15] Li, X. *et al*. Background limited ultraviolet photodetectors of solar-blind ultraviolet detection. *Appl. Phys. Lett*. **103**, 171110 (2013). https://doi.org/10.1063/1.4826458

[16] Tao, J. *et al*. Organic UV-sensitive phototransistors based on distriphenylamineethynylpyrene derivatives with ultra-high detectivity approaching 10^{18}. *Adv. Mater*. **32**, 1907791 (2020). https://doi.org/10.1002/adma.201907791

[17] Song, I. *et al*. High-performance visible-blind UV phototransistors based on n-type naphthalene diimide nanomaterials. *ACS Appl. Mater. Interfaces* **10**, 11826−11836 (2018). https://doi.org/10.1021/acsami.8b01500

[18] Qi, Z., Cao, J., Li, H., Ding, L. & Wang, J. High-performance thermally stable organic phototransistors based on PSeTPTI/$PC_{61}BM$ for visible and ultraviolet photodetection. *Adv. Funct. Mater*. **25**, 3138–3146 (2015). https://doi.org/10.1002/adfm.201500525

[19] Han, T. *et al*. Ultrahigh photosensitive organic phototransistors by photoelectric dual control. *J. Mater. Chem. C* **7**, 4725–4732 (2019). https://doi.org/10.1039/c9tc00324j

[20] Yang, B. *et al*. High performance ternary organic phototransistors with photoresponse up to 2600 nm at room temperature. *Adv. Funct. Mater*. **31**, 2103787 (2021). https://doi.org/10.1002/adfm.202103787

[21] Bianconi, S., Lauhon, L. J. & Mohseni, H. Exaggerated sensitivity in photodetectors with internal gain. *Nat. Photonics* **15**, 714 (2021). https://doi.org/10.1038/s41566-021-00843-6

[22] Rogalski, A. Detectivities of WS_2/HfS_2 heterojunctions. *Nat. Nanotechnol.* **17**, 217–219 (2022). https://doi.org/10.1038/s41565-022-01076-6

[23] Rogalski, A. Overestimating the performance of photon ultraviolet detectors. *IEEE Electron Device Lett*. **44**, 805–808 (2023). https://doi.org/10.1109/LED.2023.3262000

[24] Wang, F., Zhang, T., Xie, R., Wang, Z. & Hu, W. How to characterize figures of merit of two-dimensional photodetectors. *Nat. Commun*. **14**, 2224 (2023). https://doi.org/10.1038/s41467-023-37635-1

[25] Shan, T., Hou, X., Yin, X. & Guo, X. Organic photodiodes: device engineering and applications. *Front. Optoelectron*. **15**, 49 (2022). https://doi.org/10.1007/s12200-022-00049-w

[26] Natali, D. & Caironi, M. Organic Photodetectors. in *Photodetectors. Materials, Devices and Applications* (ed. Nabet, B.) 197–254 (Elsevier, Amsterdam, 2016). https://doi.org/10.1016/B978-1-78242-445-1.00007-5

[27] Sandberg, O. J. *et al*. Mid-gap trap state-mediated dark current in organic photodiodes. *Nat. Photonics* **17**, 368–374 (2023). https://doi.org/10.1038/s41566-023-01173-5